CHARACTERIZATION OF THE OPTICAL PROPERTIES OF GALLIUM ARSENIDE AS A FUNCTION OF PUMP INTENSITY USING PICOSECOND ULTRASONICS

By

Vimal Deepchand

Thesis

Submitted to the Faculty of the

Graduate School of Vanderbilt University

in partial fulfillment of the requirements

for the degree of

MASTER OF SCIENCE

In

Physics

May, 2010

Nashville, Tennessee

Approved:

Professor Norman H. Tolk

Professor Kalman Varga

TABLE OF CONTENTS

Page

LIST OF FIGURES ... iii

Chapter

I. INTRODUCTION ... 1

II. CAP THEORY ... 2

2.1 Strain Generation ... 2

III. TYPICAL PUMP-PROBE SETUP ... 10

IV. CAP EXPERIMENT ON GALLIUM ARSENIDE ... 12

4.1 Sample fabrication ... 12
4.2 Experimental procedure ... 12
4.3 Modeling the experimental response ... 15

V. RESULTS AND DISCUSSION ... 17

5.1 Amplitude of oscillations ... 18
5.2 Phase and period of oscillations ... 19

VI. FUTURE PLANS ... 23

REFERENCES ... 25

LIST OF FIGURES

Figure Page

1. Schematic diagram of a pump-probe technique 2
2. Spatial strain as a function of depth into the sample 4
3. Effect of thermal conduction on the shape of the acoustic pulse at different values of the thermal diffusivity 6
4. A typical pump-probe experimental configuration 10
5. Reflectivity curve obtained at a pump power of 30 mW at a wavelength of 880 nm 13
6. Subtracted oscillatory response obtained at 30 mW pump power fitted with a damped oscillatory model 14
7. Traveling CAP wave into the sample and interference of reflected probe beams 15
8. Net transient reflectivity curve as a function of pump power 17
9. Amplitude of oscillations as a function of pump intensity 18
10. Period of oscillations as a function of intensity 19
11. Phase of oscillations as a function of intensity 20
12. Reflectivity curves obtained on GaSb/GaAs at different wavelengths 21

CHAPTER I

INTRODUCTION

Picosecond ultrasonics has been used to study coherent acoustic phonon (CAP) oscillations generated by ultrafast optical excitation in various material systems. In these experiments, coherent phonons are generated from the absorption of femtosecond laser pump light pulses at the surface[1-5]. The coherent phonons modulate the optical properties of samples such as reflectance and transmittance, which are monitored by using time-delayed probe pulses. Traveling CAP waves have also been observed in III-V semiconductors and some magnatites[6-8]. In these experiments, photo-induced CAP waves generated near the surface travel into the substrate following excitation. The subsequent interference between the probe laser photons reflected from the surface and the traveling coherent longitudinal phonon plane wave results in oscillations in the pump-probe reflectance responses. These oscillations are in contrast to the observed short lived, fast oscillations arising from the coherent optical phonon modulations of the optical properties of the near surface.

In this thesis, we describe pump beam-intensity-dependence measurements on GaSb(20 nm)/GaAs at room temperature. The pump wavelength was set to 880 nm, which is slightly below the band gap of GaAs at room temperature, to ensure a strong oscillatory response as reported by Miller *et al.*[9] and Xu *et al*[10]. We also present a discussion of a theory behind CAP generation in semiconductors, and use it to explain what we observe in our experiments. We suggest that our technique is a non-invasive means of characterizing the optical properties of GaAs and point out that further modeling of our results is possible and imminent.

CHAPTER II

CAP THEORY

2.1 Strain Generation

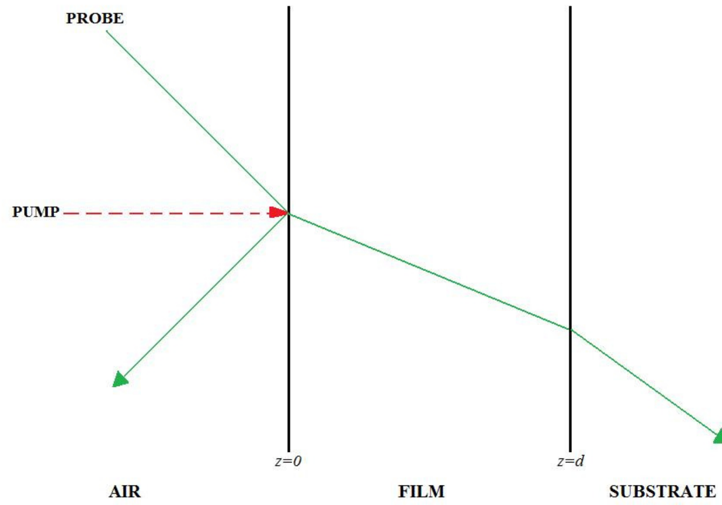

Figure 1: Schematic diagram of a typical pump-probe experiment. A pump pulse is directed onto the sample at near normal incidence and a probe beam is shone on the same spot. The reflected probe beam contains information about reflectivity changes induced by the incident pump beam.

Figure 1 shows a short light pulse of duration $\tau_0 < 1$ ps and energy Q incident on the free surface of a film of thickness d. Thomsen *et al.*[1] assumed that d was much larger than the absorption length ζ and that much smaller than the linear dimension of the area A. The total energy deposited per unit volume at a depth z into the film from the free surface is given by

$$W(z) = (1 - R)\frac{Q}{A\zeta}e^{-z}/\zeta \qquad (1)$$

where R is the reflectivity. This causes a temperature increase of

$$\Delta T(z) = \frac{W(z)}{C} \tag{2}$$

where C is the specific heat per unit volume. This temperature increase creates an isotropic thermal stress which, in terms of the bulk modulus B and the linear expansion coefficient β, is given by

$$-3B\beta\Delta T(z) \tag{3}$$

Assuming the film to be elastically isotropic, the only motion that needs to be considered is the one along the z direction since the stress would depend only on z. Therefore, η_{33} is the only non-vanishing component of the elastic strain tensor. The elastic equations that need to be solved are therefore

$$\sigma_{33} = 3\frac{1-\nu}{1+\nu}B\eta_{33} - 3B\beta\Delta T(z) \tag{4}$$

$$\rho\frac{\partial^2 u_3}{\partial t^2} = \frac{\partial \sigma_{33}}{\partial z} \tag{5}$$

$$\eta_{33} = \frac{\partial u_{33}}{\partial z} \tag{6}$$

where ν is the Poisson ration, ρ the density and u_3 the displacement along the z direction. Using the condition that the strain is initially zero everywhere, and that the stress σ_{33} is zero at the free surface, the solution is

$$\eta_{33}(z,t) = (1-R)\frac{1+\nu}{1-\nu}[e^{-\frac{z}{\zeta}}\left(1-\frac{1}{2}e^{-\frac{vt}{\zeta}}\right) - \frac{1}{2}e^{-|z-vt|/\zeta}\mathrm{sgn}(z-vt)] \tag{7}$$

where v, the longitudinal sound velocity, is given by

$$v^2 = 3\frac{1-\nu}{1+\nu}\frac{B}{\rho} \tag{8}$$

To arrive at equation (7), Thomsen *et al.*[1] assumed that the area heated by the pulse was much larger than the film thickness d so that ΔT, σ and η would depend only on z. They showed that this assumption was valid for their experiments in a near field region defined by

$$Z \sim \frac{w^2}{\zeta} \tag{9}$$

where w is of the same order as the linear dimensions of the heated region. Secondly, they also assumed that the temperature rose instantaneously to its maximum value after which it remained constant. Their experiments showed that this assumption holds well in the regime where the distance travelled by the strain pulse during the pulse duration τ_0 is much smaller than the absorption length:

$$v\tau_0 \ll \zeta \tag{10}$$

Figure 2 shows the strain given by equation (7).

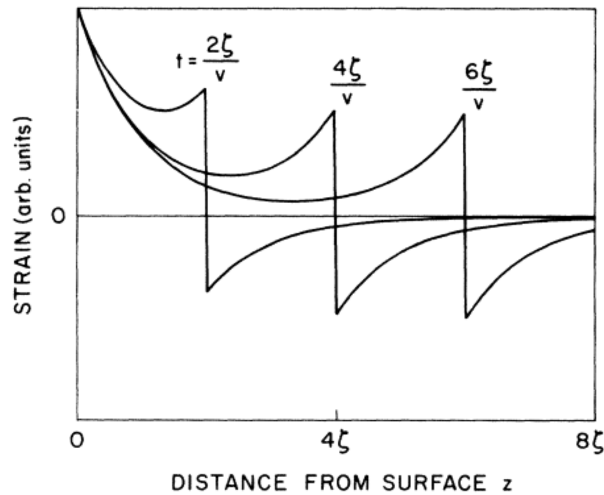

Figure 2[1]: The spatial strain as a function of the distance z from the surface at different times. Note that the stress pulse is propagating to the right, causing the strain to be negative ahead of it, a positive behind it.

Taking into account the effect of heat diffusion after the light pulse is absorbed, Thomsen *et al.* derived a new expression for the strain pulse which has a contribution from two strain pulses, one traveling in the negative *z* direction (which gets reflected off the free surface) and one traveling towards the positive *z* direction:

$$\eta_{33}(z,t) = (1-R)\frac{QB}{A\zeta C}\frac{1+\nu}{1-\nu}F(z-vt) \quad (11)$$

The function *F* governs the shape of the pulse. For $z > vt$,

$$F(z-vt) = -\frac{1}{2}e^{-(z-vt)/\zeta} - \frac{1}{2}\int_{0+}^{\infty} dt' \int_{0}^{\infty} dz' \frac{\partial\Theta(z',t')}{\partial t'}\delta\left(z' - z + v(t-t')\right) \quad (12)$$

For $z < vt$,

$$F(z-vt) = \frac{1}{2}e^{-(z-vt)/\zeta} - \frac{1}{2}\int_{0+}^{\infty} dt' \int_{0}^{\infty} dz' \frac{\partial\Theta(z',t')}{\partial t'}[\delta\left(z' - z + v\left(t-t'\right)\right) - \delta\left(z' + z + v\left(t-t'\right)\right) \quad (13)$$

Here,

$$\Theta(z,t) = \int_{-\infty}^{\infty} dz'(4\pi Dt)^{-1/2}e^{-\left(z-z'\right)^2/4Dt}e^{-|z'|/\zeta} \quad (14)$$

and *D* is the thermal diffusivity (*D* = *K/C*, *K* is the thermal conductivity). The function *F* is shown in figure 3.

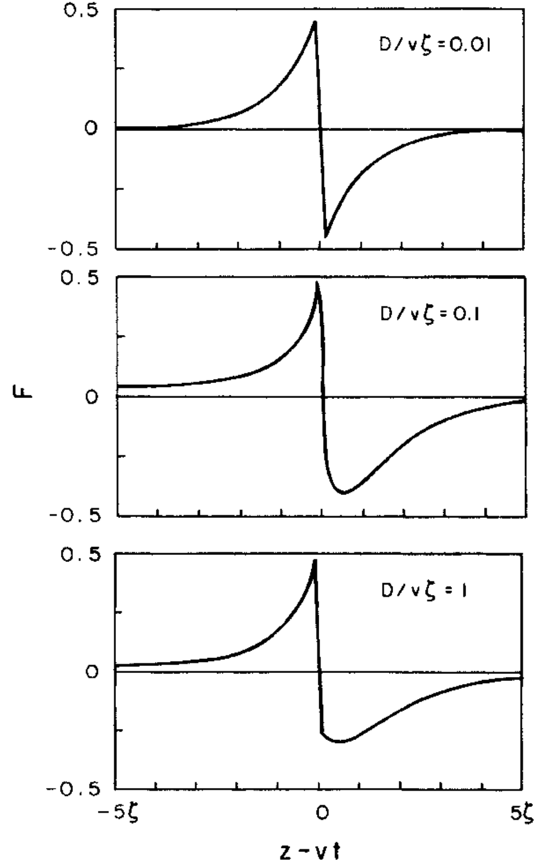

Figure 3: The effect of thermal conduction on the shape of the acoustic pulse for different values of D, as modeled by Thomsen *et al.*[1]

A more general treatment of the generation process takes into account how the light pulse changes the electron and phonon distributions $n_e(\boldsymbol{k})$ and $n_p(\boldsymbol{k})$ respectively, which produces a stress:

$$\sigma_{ij} = \sum_{\boldsymbol{k}} \delta n_e(\boldsymbol{k}) \frac{\partial E_k}{\partial \eta_{ij}} + \sum_{\boldsymbol{k}} \delta n_p(\boldsymbol{k}) \hbar \frac{\partial \omega_k}{\partial \eta_{ij}} \tag{15}$$

where $E_{\boldsymbol{k}}$ and $\omega_{\boldsymbol{k}}$ are the energy and frequency of a phonon of wavevector $\boldsymbol{k}$ respectively. In semiconductors, light pulses produce electron-hole pairs. The electron-hole contribution to the stress is

$$\sigma_{ij}^{e} = \frac{\partial E_g}{\partial \eta_{ij}} \delta n_e = -B \frac{dE_g}{dP} \delta_{ij} \delta n_e \tag{16}$$

This equation assumes elastic isotropy. E_g is the band gap energy, δn_e is the number of electrons (identical to the number of holes) and P is the pressure.

Light of energy E produces thermal phonons of energy $(E\text{-}E_g)$. Assuming these phonons follow a thermal distribution, the phonon contribution to the stress is

$$\sigma_{ij}^{p} = -\frac{3B\beta}{C} (E - E_g) \delta_{ij} \delta n_e \tag{17}$$

In short, Thomsen *et al.*[1] have shown that a pump beam shone onto a sample generates a stress pulse which propagates in that sample.

A strain pulse created by the incident light ray changes the optical constants of the film, causing the reflectivity to change by ΔR when the strain is pulse is close to the surface. The strain causes the real and imaginary parts of the refractive index to change by

$$\Delta n(z,t) = \frac{\partial n}{\partial \eta_{33}} \eta_{33}(z,t) \tag{18}$$

$$\Delta \kappa(z,t) = \frac{\partial \kappa}{\partial \eta_{33}} \eta_{33}(z,t) \tag{19}$$

The imaginary part of the refractive index, the extinction coefficient κ, indicates the amount of light absorbed when they propagate through the material and is related to the absorption coefficient:

$$\alpha = \zeta^{-1} = \frac{2\omega\kappa}{c} \tag{20}$$

Consider a light wave at normal incidence with the electric field. In the presence of strain, we need to solve Maxwell equations inside the film to find out the changes in reflectivity due to the strain. We have to solve

$$\frac{\partial^2 \mathcal{E}_x}{\partial z^2} = -\frac{\omega^2}{c^2}[\epsilon + \Delta\epsilon(z,t)]\mathcal{E}_x(z) \tag{21}$$

where $\Delta\epsilon(z,t)$ is the change in the dielectric constant ϵ caused by the strain and

$$\epsilon = (n + i\kappa)^2 \tag{22}$$

Assuming that the strain exists only at a certain distance *z'* from the interface, i.e.,

$$\Delta\epsilon = F\delta(z - z') \tag{23}$$

the strain creates a discontinuity at $z = z'$ which reflects part of the wave transmitted through the film. The reflection coefficient can be found from (23):

$$r_1 = \frac{ik_0^2}{2k}F \tag{24}$$

where k_0 and k are the wave vectors in vacuum and the film respectively. The reflected wave is then transmitted into vacuum and the transmission coefficient is

$$\tilde{t}_0 = \frac{2k}{k_0 + k} \tag{25}$$

The total reflected wave is

$$\mathcal{E}_x^{(r)} = \left(r_o + t_0 r_1 \tilde{t}_0 e^{2ikz'}\right)\mathcal{E}_0 e^{i(-k_0 z - \omega t)} \tag{26}$$

where $\mathcal{E}_0$ is the amplitude of the electric field incident from vacuum on the interface and r_0 is the reflection coefficient from vacuum into the film.

Using these results and further simplifying, Thomsen *et al.*[1] derived an expression for the change in reflectivity to first order in strain:

$$\Delta R(t) = \int_0^\infty f(z)\eta_{33}(z,t)dz \tag{27}$$

where

$$f(z) = f_0 \left[\frac{\partial n}{\partial \eta_{33}} \sin\left[\frac{4\pi n z}{\lambda} - \phi\right] + \frac{\partial \kappa}{\partial \eta_{33}} \cos[\frac{4\pi n z}{\lambda} - \phi]\ \right] e^{-z/\zeta} \tag{28}$$

$$f_0 = 8\,\frac{\omega\left[n^2\left(n^2+\kappa^2-1\right)^2+\kappa^2\left(n^2+\kappa^2+1\right)^2\right]^{1/2}}{c[(n+1)^2+\kappa^2]^2} \tag{29}$$

$$\tan\phi = \frac{\kappa(n^2+\kappa^2+1)}{n(n^2+\kappa^2-1)} \tag{30}$$

The sensitivity function *f* determines how the strain at different depths changes the reflectivity. The general form of *f* is an exponentially-damped oscillation with a non-zero phase at the surface, with a periodicity equal to half that of the wavelength of the light in the film and a range determined by the absorption length ζ of the light[1].

A similar approach can be used to work out the change in transmittivity. As evidenced by equation (27), Thomsen *et al.*[1] showed that a strain in the sample causes a change in reflectivity. This change can be monitored, as described in chapter IV.

CHAPTER III

TYPICAL PUMP-PROBE SETUP

Figure 4 shows a pump probe experimental setup used to measure reflectivity changes in a typical pump-probe experiment.

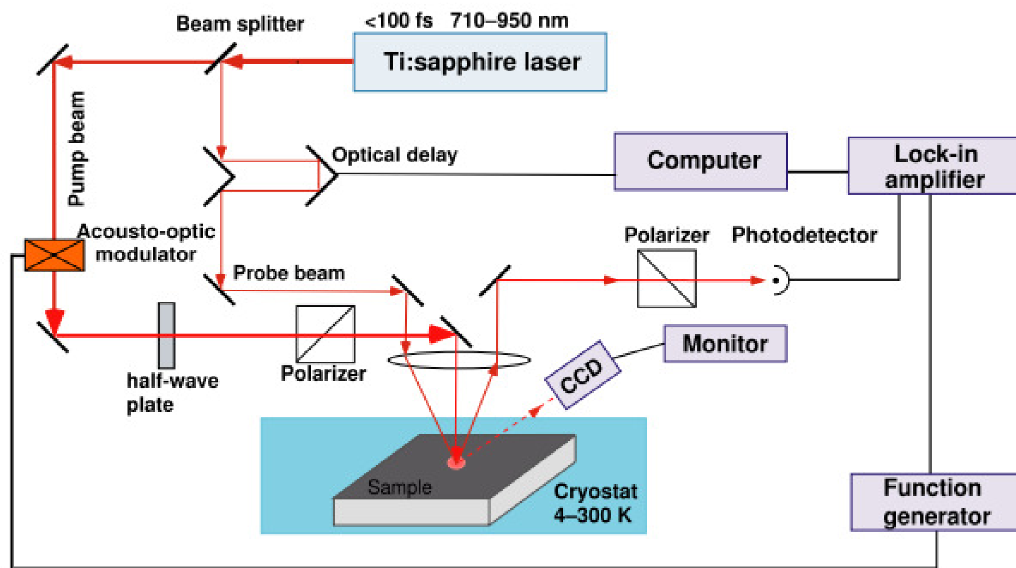

Figure 4: A typical pump-probe experimental configuration

The output of a Ti:sapphire laser is split into a pump beam and a probe beam . The pump beam excites the sample and changes its optical properties and reflectivity. The incident probe beam modifies the reflectivity changes ΔR induced by the pump beam and the reflected probe beam gets detected. To minimize the impact of the probe beam on the optical properties of the sample, the probe beam power is much smaller than the pump beam power (usually by at least a factor of 10). The polarizers in the paths of the

pump and probe beams (which may be of the same wavelength) cause these beams to be cross-polarized. Hence, they do not interfere at the detector and the polarizer in front of the detector may be adjusted to let in the reflected probe beam only. An optical delay mechanism changes the path length of the probe beam and causes the probe beam to reach the sample at different times after the pump pulse has struck the sample. A function generator controls the frequency at which the acouto-optic modulator (AOM) modulates the pump beam and feeds the same frequency to the lock-in amplifier. The lock-in amplifier may therefore be used to optimize the detection of the very small ΔR using lock-in techniques.

CHAPTER IV

CAP EXPERIMENT ON GALLIUM ARSENIDE

4.1 Sample fabrication

A GaSb/GaAs sample was used. The sample is grown using molecular beam epitaxy (MBE). A (001) GaAs substrate is heated to 600^0C under As_2 flux to remove oxidation. A 100 nm GaAs buffer layer is then grown on the substrate at GaAs growth condition (~ 600^0C). Finally, a capping layer of GaSb of thickness 20 nm is grown at 480^0C.

4.2 Experimental Procedure

A 76 MHz Mira 900 Ti:sapphire laser with a pulse width of 150 fs was used to perform standard femtosecond time-resolved optical pump-probe measurements on the transient reflectivity change $\Delta R/R$ on the sample at room temperature. Pump pulses ranging between 10 mW and 110 mW in power were used to optically excite charge carriers in the GaSb layer. A fixed probe power of 3 mW was used to monitor the reflectivity changes. The pump and probe wavelengths were both kept at 880 nm.

The pump beam was shone at near-normal incidence on the sample. The angle of incidence of the probe beam with the sample was ~ 5^0. Figure 5 shows the total response for a pump power of 30 mW.

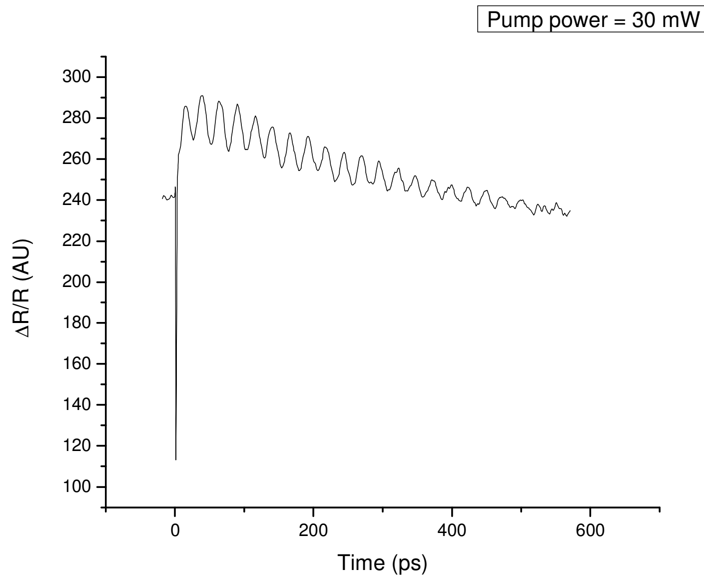

Figure 5: Total pump-probe response of GaSb(20 nm)/GaAs at 880 nm at 300 K obtained at a pump power of 30 mW in our experiments

The total response is made up of a fast transient (of the order of a few ps) followed by a long-lasting damped oscillatory tail. The initial transient occurs due to the excitation of hot photoexcited electron-hole pairs and relaxation through electron-phonon interaction in GaSb. The long-lasting damped oscillatory tail is not directly related to the pump beam since it only occurs after the transient[9,10]. The measured response in figure 6 is obtained by subtracting the thermal relaxation background from the total response (open triangles) and is fitted with an exponentially damped function (solid line).

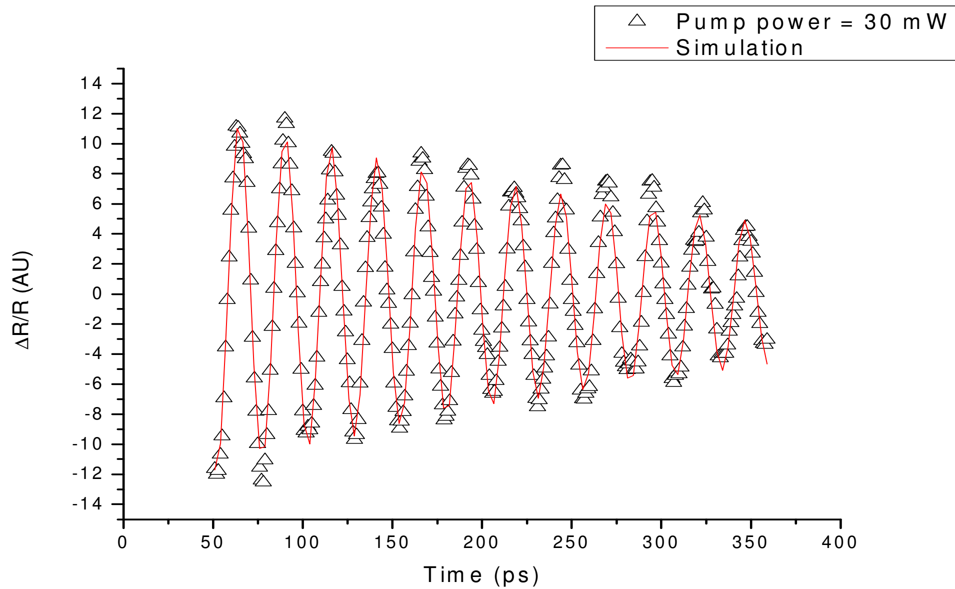

Figure 6: The subtracted oscillatory response at 30 mW pump power (open triangles) fitted with a damped oscillation model (solid line).

The Thomsen model described in section 2 can be used to explain the origin of this class of oscillations. The pump pulse ($\lambda = 880$ nm, E =1.4 eV) is absorbed by the top GaSb layer (band gap = 0.8 eV). This leads to a transient electron and phonon temperature increase within the illuminated area, which in turn sets up a transient stress. The transient stress induces a strain wave or coherent acoustic phonons (CAP) which propagates away from the sample surface at the speed of longitudinal acoustic (LA) phonons. The CAP modifies the local dielectric constant and creates a local discontinuity. The probe light partially reflects off the top surface and partially transmits through the substrate and reflects off the discontinuity. The discontinuity (strain wave) and the top surface act as interferometers [figure 7].

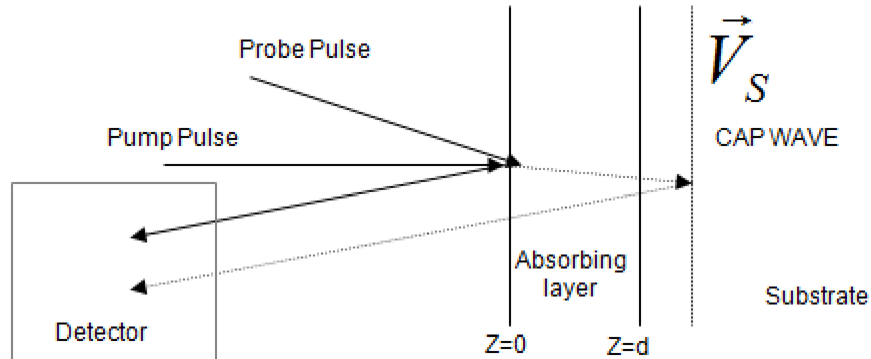

Figure 7: A CAP wave traveling to the right with longitudinal sound velocity $\vec{V_S}$ inside the substrate. Part of the incident probe beam reflects off the absorbing layer, and the rest transmits through the substrate and reflects off the traveling strain pulse. The 2 reflected beams interfere with each other and are detected at the detector.

Oscillations arise because the distance between the two surfaces changes, resulting in a periodic phase difference between the 2 reflected beams[9,11].

The band gap of GaAs (1.5 eV) is very close to the photon energy. The photon energy is about 5 times more strongly absorbed in GaSb (band gap = 0.8 eV) than in GaAs[12]. In our experiment, it can therefore be assumed that the only the GaSb layer absorbs the photon energy.

4.3 Modeling the Experimental Response

The transfer of the excess energy of photoexcited carrier in GaSb to the bulk creates a strained layer that propagates away from the surface with LA phonon velocity V_s. The overall measured signal is the sum (interference) of the probe beam reflected off the air/bulk interface and the probe beam reflected off the bulk/strained layer boundary at a distance $z = V_S t$. In this three-layer system, the reflection coefficient is

$$R = \left|\frac{r_{12}+r_{23}e^{2ikz}}{1+r_{12}r_{23}e^{2ikz}}\right|^2 \tag{31}$$

where $r_{ij} = \frac{N_i - N_j}{N_i + N_j}$ is the Fresnel reflection amplitude from the boundary between media *i* and *j*, and N_i is the complex index of refraction of media *i*. Here, $N_1 = 1$ for air, $N_2 = N(\omega) = n(\omega) + i\kappa(\omega)$ for the bulk semiconductor (GaAs) and $N_3 = N(\omega) + \delta N(\omega)$ in the strained layer. Therefore, r_{12} and $r_{23} \sim \delta N/N$ are the reflection amplitudes from the air/bulk and bulk/strain interfaces. Since δN, the strain-induced change in refractive index, is very small, equation (31) can be expanded to first order in small parameter r_{23}. The differential reflection $\frac{\Delta R}{R_0} = \frac{R - R_0}{R_0}$, where $R_0 = |r_{12}|^2$ is therefore given by

$$\frac{\Delta R}{R_0} \approx A e^{-t/\tau} \sin\left(\frac{2\pi t}{T} + \phi\right) \tag{32}$$

where $A \propto \delta N/N$ is the amplitude, ϕ is the phase and *T* is the period. T can be shown to be

$$T = \lambda/2nV_s \cos\theta \tag{33}$$

where λ is the probe wavelength in air, *n* is the index of refraction in GaAs, V_s is the speed of LA phonons and θ is the angle of incidence of the probe light in GaAs.

The damping time τ is given by

$$\tau = \frac{\lambda}{4\pi\kappa V_s \cos\theta} = \frac{Tn}{2\pi k} \tag{34}$$

CHAPTER V

RESULTS AND DISCUSSION

The oscillatory response at 880 nm at different pump powers is shown in figure 8.

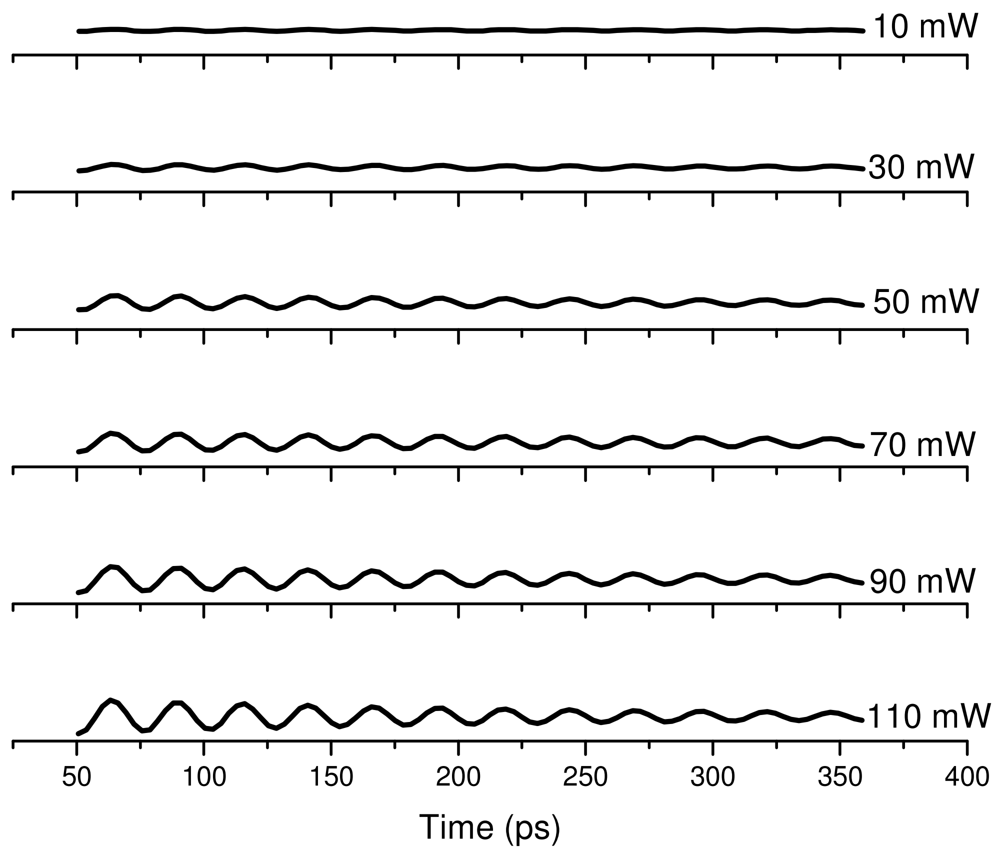

Figure 8: Some oscillatory responses ($\Delta R/R$) at 880 nm and room temperature obtained at different pump powers from our experiments. The pump power for each curve is shown to its right. The amplitude of the oscillations increases at higher pump powers. The time t=0 ps is when the pump and the probe beam strike the GaSb surface at the same time.

The curves in figure 8 are obtained by fitting the experimental data with equation (32). From the fitted equation, the amplitude, phase, period and decay time can be found.

5.1 Amplitude of Oscillations

In the low intensity regime of the experiment, the amplitude is found to vary linearly with pump intensity (figure 9). From (34), the amplitude of the oscillations is proportional to the change in index of refraction δN. From equations (18) and (19), δN will be proportional to the intensity of the pump beam if $\eta_{33}(z,t)$ itself is proportional to the pump intensity. This linear behavior of the strain with pump intensity can be deduced by considering the electron and phonon contributions to the stress (equations 15-17). In the low intensity regime, every photon of light creates an electron-hole pair. Therefore, δn_e will increase linearly with intensity, as will the stress from equation (15).

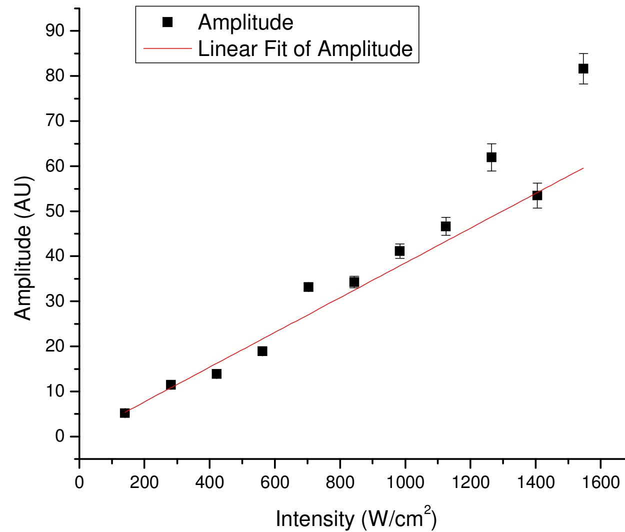

Figure 9: In our experiments, the amplitude of the oscillations is found to increase linearly with pump intensity at low intensities.

Our experiments at least show that in the low intensity regime, the stress is linearly proportional to the strain. It is likely that at higher intensities, the graph in figure 9 may saturate at higher pump intensities once the proportionality between δn_e and the intensity is lost. This particular case will be investigated using a laser source more intense than the one used in the experiments described in this thesis.

5.2 Phase and Period of Oscillations

A plot of the period of oscillations versus time at different powers shows that the period is unaffected by the change in pump intensity in our experiments (figure 10). This result is consistent with equation (33):

$$T = \lambda/2nV_s \cos\theta \tag{33}$$

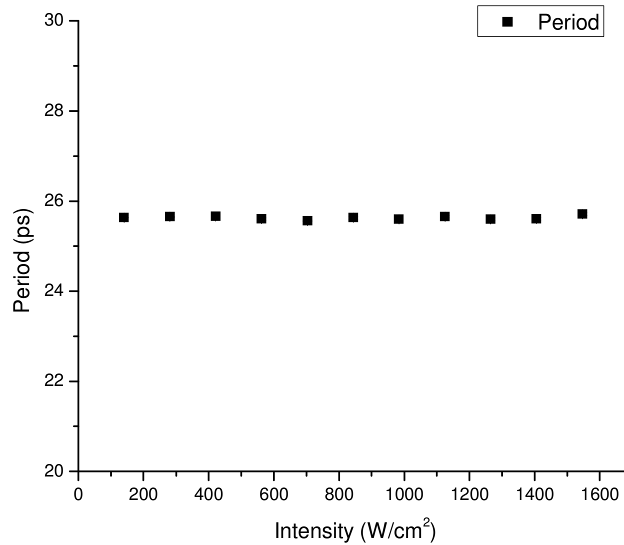

Figure 10: The period remains constant at different intensities. From our experimental data, the average period is determined to be 26.2 ps ± 0.1 ps.

In the low intensity regime of this experiment, the phase of the oscillations was also found to be constant (figure 11).

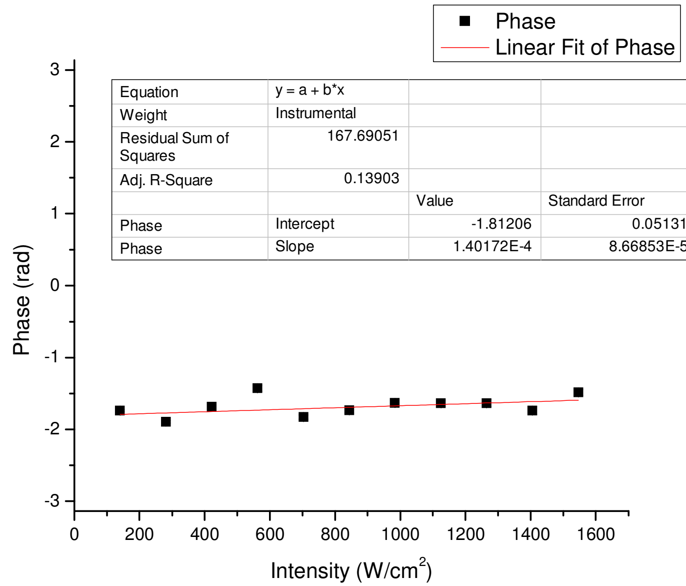

Figure 11: The phase of the oscillations in our experiments does not change with pump intensity.

In this experiment, the GaSb layer was assumed to be thin enough so that no CAP oscillations exist in it. However, CAP oscillations become significant in thicker GaSb layer and have been reported previously[6,9]. Figure 12 indicates the presence of CAP waves in a 500 nm thick GaSb layer, reported by Miller *et al*[9].

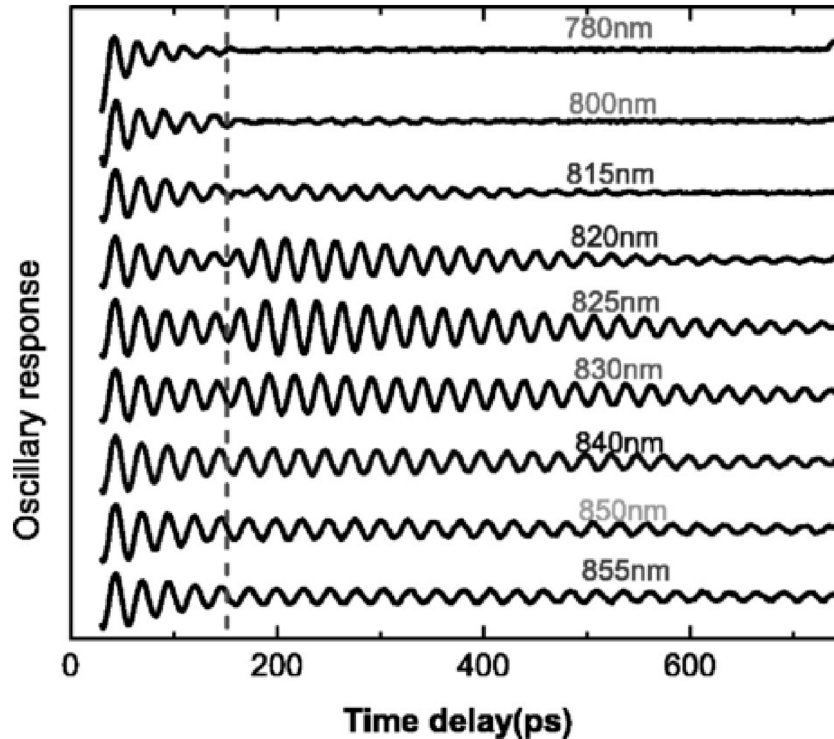

Figure 12: CAP studies in GaSb (500nm)/GaAs at different wavelengths (Miller *et al.*[9]). The dash line indicates the time when the strain wave travels through the bulk GaAs. The variation of the phase of the oscillations in GaAs with wavelength is visible and expected since the period of oscillations changes with pump wavelength.

Miller *et al.*[9] used a fixed GaSb film thickness and varied the pump wavelength, which caused the period of oscillations to vary which in turned changed the phase of the oscillations in GaAs. It is conceivable that at a fixed wavelength and pump intensity and varying GaSb film thicknesses, the onset of the oscillations – and hence their phases - in the GaAs bulk will be determined by the GaSb film thickness. Our current intensity-dependent measurements indicate that the period of oscillations does not change – and neither does the phase – with pump intensity, in the low intensity regime. Therefore, it is very likely that in the low intensity regime of our experiments, the thickness of GaSb is constant. It is anticipated that at higher pump laser intensities, a sufficiently large thermal expansion of the GaSb layer may produce a noticeable shift in the phase of oscillations.

Higher laser pump intensities can be achieved using an optical parametric oscillator (OPA).

CHAPTER VI

FUTURE PLANS

In summary, we have carried out systematic intensity-dependent studies of traveling CAP waves in GaSb/GaAs using time-resolved pump-probe reflectance measurements. An oscillatory response, attributed to the interference between the reflected probe beams off the GaSb layer and the traveling strain layer due to a "Fabry-Pérot" interferometer configuration, has been observed in GaAs. We have suggested a model to explain the linear relationship between the amplitude of the oscillatory signal in terms of changing free carrier concentration and noted that this relationship may fail at very high intensities due to the saturation of free charge carrier concentration. Furthermore, the amplitude of the oscillations has also been shown to be related to the change in index of refraction of GaAs due to the presence of a traveling strain pulse in it, indicating intensity dependent studies as a potential means to characterize the strain field in the GaAs.

Ongoing effort on this area also involves developing a model that will enable us to analytically spatially map out the strain pulses at different pump pulse intensities. Similar endeavors on mapping out the strain field have been recently done by Liu *et al*[13] and Tomoda *et al*[14] who performed experiments on glass and piezoelectric InGaN/GaN heterostructures respectively. Furthermore, Wu *et al.*[15] developed a theoretical model to simulate the strain pulse in single crystal bulk GaN which enabled them to predict the dominant mechanism of CAP generation in their sample. Developing a model suited for our work holds the promise to further understand the microscopic activities in play at

different pump intensities in our samples, as well as quantifying physical and optical properties such as density and refractive index of the traveling strain pulse.

The phase of the oscillations has also been studied and found to be constant at low intensities. If thermal expansion of the capping GaSb layer becomes significant at higher pump intensities, the phase of the oscillations is expected to change and this remains to be studied. In that light, we propose to perform CAP experiments on GaSb/GaAs as a function of varying GaSb layer thicknesses at fixed pump intensity. The phase of oscillations obtained in these experiments would then be compared with the phase obtained by varying the pump intensity in experiments on a single, specific GaSb/GaAs sample. If it is found that the period of CAP oscillations in GaAs does not change with intensity, even at intensities higher than the ones employed in this work, the aforementioned proposed experiments may provide a useful means of gauging the thermal expansion of the GaSb layer.

Future related work will necessarily involve studies at pump intensities higher than the ones used in the experiments described in this report, achievable through the use of an optical parametric oscillator (OPA), to non-invasively investigate the optical properties of GaAs.

REFERENCES

1. C. Thomsen, H. T. Grahn, H. J. Maris, and J. Tauc, *Surface generation and detection of phonons by picosecond light pulses*, Phys. Rev. B **34**, 4129 (1986).

2. T. Pfeifer, W. Kutt, H. Kurz, and R. Scholz, *Generation and detection of coherent optical phonons in germanium,* Phys. Rev. Lett. **69**, 3248 (1992).

3. C. Sun, J. C. Liang, and X. Y. Yu, *Coherent Acoustic Phonon Oscillations in Semiconductor Multiple Quantum Wells with Piezoelectric Fields*, Phys. Rev. Lett. **84**, 179 (2000).

4. I. Bozovic, M. Schneider, Y. Xu, R. Sobolewski, Y. H. Ren, G.Lupke, J. Demsar, A. J. Taylor, and M. Onellion, *Long-lived coherent acoustic waves generated by femtosecond light pulses*, Phys. Rev. B **69**, 132503 (2004).

5. M. Hase, K. Ishioka, J. Demsar, K. Ushida, and M. Kitajima, *Ultrafast dynamics of coherent optical phonons and nonequilibrium electrons in transition metals*, Phys. Rev. B **71**, 184301 (2005).

6. J. Wang, Y. Hashimoto, J. Kono, A. Oiwa, H. Munekata, G. D. Sanders, and C. J. Stanton, *Propagating coherent acoustic phonon wave packets in* $In_xMn_{1-x}As/GaSb$, Phys. Rev. B **72**, 153311 (2005).

7. S. Wu, P. Geiser, J. Jun, J. Karpinski, J.-R. Park, and R. Sobolewski, *Long-lived, coherent acoustic phonon oscillations in GaN single crystals*, Appl. Phys. Lett. **88**, 041917 (2006).

8. J. S. Yahng, Y.D. Yho, K. J. Yee, E. Oh, J. C. Woo, D. S. Kim, G. D. Sanders, and C. J. Stanton, *Probing strained InGaN/GaN nanostructures with ultrashort acoustic phonon wave packets generated by femtosecond lasers*, Appl. Phys. Lett. **80**, 4723 (2002).

9. J. K. Miller, J. Qi, Y. Xu, Y.-J. Cho, X. Liu, J. K. Furdyna, I. Perakis, T. V. Shahbazyan, and N. Tolk, *Near-bandgap wavelength dependence of long-lived traveling coherent longitudinal acoustic phonons in GaSb-GaAs heterostructures*, Phys. Rev. B **74**, 113313(2006).

10. Y. Xu, J. Qi, J. Miller, Y.-J. Cho, X. Liu, J. K. Furdyna, T. V. Shahbazyan, N. Tolk¸ *Pump-probe studies of travelling coherent longitudinal acoustic phonon oscillations in GaAs*, Physica Status Solidi (c) **5**, 2632 (2008).

11. H.-N. Lin, R. J. Stoner, H. J. Maris, and J. Tauc, *Phonon attenuation and velocity measurements in transparent materials by picosecond acoustic interferometry*, J. Appl. Phys. **69**, 3816 (1991).

12. D. E. Aspnes and A. A. Studna, *Dielectric functions and optical parameters of Si, Ge, GaP, GaAs, GaSb, InP, InAs, and InSb from 1.5 to 6.0 eV*, Phys. Rev. B **27**, 985 (1983).

13. R. Liu, C. S. Kim, G. D. Sanders, C. J. Stanton, J. S. Yahng, Y. D. Jho, K. J. Yee, E. Oh, and D. S. Kim, *Ultrafast spectroscopy of propagating coherent acoustic phonons in GaN/InGaN heterostructures*, arXiv:cond-mat/0310654 (2008).

14. M. Tomoda, R. Li Voti, O. Matsuda, and O. B. Wright, *Tomographic reconstruction of picosecond acoustic strain propagation*, Appl. Phys. Lett. **90**, 041114 (2007).

15. S. Wu, P. Geiser, J. Jun, J. Karpinski, and R. Sobolewski, *Femtosecond optical generation and detection of coherent acoustic phonons in GaN single crystals*, Phys. Rev. B **76**, 085210 (2007).